Nuclear Engineering and Technology 53 (2021) 266–272

Contents lists available at ScienceDirect

Nuclear Engineering and Technology

journal homepage: www.elsevier.com/locate/net

Original Article

Development of a neural network method for measuring the energy spectrum of a pulsed electron beam, based on Bremsstrahlung X-Ray

Mohsen Sohrabi, Navid Ayoobian, Babak Shirani*

Faculty of Physics, University of Isfahan, 8174673441, Isfahan, Iran

ARTICLE INFO

Article history:
Received 31 May 2019
Received in revised form
9 June 2020
Accepted 30 June 2020
Available online 9 July 2020

Keywords:
Pulsed electron beam
Neural network
Multilayer perceptron
MCNP

ABSTRACT

In the pulsed electron beam generators, such as plasma focus devices and linear induction accelerators whose electron pulse width is in the range of nanosecond and less, as well as in cases where there is no direct access to electron beam, like runaway electrons in Tokamaks, measurement of the electron energy spectrum is a technical challenge. In such cases, the indirect measurement of the electron spectrum by using the bremsstrahlung radiation spectrum associated with it, is an appropriate solution. The problem with this method is that the matrix equation between the two spectrums is an ill-conditioned equation, which results in errors of the measured X-ray spectrum to be propagated with a large coefficient in the estimated electron spectrum. In this study, a method based on the neural network and the MCNP code is presented and evaluated to recover the electron spectrum from the X-ray generated by collision of the electron beam with a target. Multilayer perceptron network showed good accuracy in electron spectrum recovery, so that for the X-ray spectrum with errors of 3% and 10%, the network estimated the electron spectrum with an average standard error of 8% and 11%, on all of the energy intervals.

1. Introduction

The energy spectrum of electrons in devices such as plasma focus, short pulse accelerators and Tokamaks contains valuable technical and scientific information. Therefore, it is important to develop measurement methods, which are compatible with requirements of a specific device such as electron pulse width, energy range, beam current and structural limitations of the device. In cases where direct electron spectroscopy is possible, lithium drift detectors and scintillators are used, however in high energy content and high current pulsed electron generators, direct measurement of electron spectrum is difficult due to the very short duration of electron pulse, as well as the destructive effects of collision of intense electron beam with the detector surface [1–6].

Plasma focus devices, as high-current, short-duration pulsed electron generators have been taken into consideration by researchers in this field, due to the complexity of electron spectroscopy in these devices [1–6].

So far, many researches have been conducted on the finding of the electron spectrum in plasma focus devices. In some of the studies, the electron spectrum was measured using a magnetic spectrometer. Kwiatkowski et al. obtained an electron energy spectrum for the PF-1000 machine between 40 and 800 keV by a magnetic analyzer [7].

Efforts were made by Patran et al. to construct an electron magnetic analyzer to record the energy spectrum of electron pulses generated by a plasma focus device [1,8,9]. This spectrometer was successfully tested on the 3 kJ plasma focus device and the energy range of the generated electron beams was measured between 30 and 660 keV.

Stygar et al. estimated the distribution of electron energy between 20 and 500 keV by using arrays of Faraday cups and a magnetic spectrometer. They also found that the distribution of the electron energy was proportional to $E^{-3.5\pm0.5}$ [10]. Neog et al. used a combination of Faraday cups and Rogowski coil to measure the electron spectrum of a plasma focus device. The electron energy distribution was obtained between 10 and 200 keV. The highest intensity of electron was also evaluated in the energy range of 80–110 keV [11].

Surala et al. reported the results of experimental studies on

* Corresponding author.
E-mail address: b.shirani@ast.ui.ac.ir (B. Shirani).

https://doi.org/10.1016/j.net.2020.06.033

pulsed electron beams of PF-360 device using two separate magnetic analyzers. This analyst was able to record electrons in channels with energies ranged in 41–715 keV [12].

In some of the studies, the Bremsstrahlung X-ray generated due to collision of electron beam with a target was used as an indirect method for measurement of electron spectrum. In plasma focus device, collision of electrons with surface of anode is the main mechanism of hard X-ray generation. Paassen et al. estimated the electron spectrum of a plasma focus device by measurement of hard X-ray emission. X-ray spectrum was measured by registration of electron tracks in a nuclear emulsion. They found that electron spectrum is extended up to 350 keV and the spectrum follows $E^{-3.3}$ distribution function [13]. Johns et al. developed a numerical formulation method to unfold the electron spectrum using hard X-ray spectrum [14].

Shamsian et al. used a method for determination of electron spectrum, based on the Bremsstrahlung spectrum measurement. In the proposed method, the matrix equation was obtained between the electron spectrum and the X-ray spectrum using the superposition principle. The coefficients matrix of this equation was calculated by simulating the problem by MCNP code. Considering the error propagation while solving matrix equations in this method, it is not possible to calculate the spectrum in more than 4 or 5 intervals with high accuracy, and this is a big problem with this method [15].

The neural network tool is nowadays a very useful tool and is used in many problems. Sharghi et al. used a neural network technique to recover the Am–Be neutron spectrum measured by the NE213 liquid scintillator detector. The result had a good consistency with the FORIST code [16].

This paper presents a method for obtaining the energy spectrum of a pulsed electron beam by the spectrum of Bremsstrahlung radiation resulting from the collision of the electrons with a target using an artificial neural network called multilayer perceptron. The required data set for training the neural network and validating this method was generated by Monte Carlo simulation of the electron-target interaction. Some of the most common Monte Carlo codes are MCNP, GEANT and FLUKA. We used the '4c' version of MCNP code for this study.

2. Methodology

2.1. Relationship between the electron spectrum and the X-ray spectrum

A single-energy electron beam after collision with a target produces an X-ray spectrum ranged from the energy of zero to the energy of the electrons. Therefore, when an electron spectrum collides with a target, an X-ray spectrum is obtained which is equal to the sum of the spectra generated by each single energy electron. In this study, the collision of pulsed electron beam to the surface of a metallic target is simulated and the X-ray spectrum measured at perpendicular direction to the direction of the electron beam is used to estimate the electron energy spectrum.

The relationship between the electron energy spectrum and the X-ray spectrum can be explained by the superposition principle. The superposition principle states that for a linear system, the net response caused by two or more stimuli is equal to the sum of the responses that would have been caused by each stimulus individually. Therefore, if the electron spectrum is divided into n intervals and the X-ray spectrum into m intervals, the X-ray spectrum amplitude at each interval will be equal to the sum of the effects of all the n individual electron intervals. In matrix statement, we have:

$$X = K \cdot E \quad \text{or} \quad \begin{bmatrix} X_1 \\ X_2 \\ \vdots \\ X_m \end{bmatrix} = \begin{bmatrix} k_{11} & k_{12} & \cdots & k_{1n} \\ k_{21} & k_{22} & \cdots & k_{2n} \\ \vdots & \vdots & \ddots & \vdots \\ k_{m1} & k_{m2} & \cdots & k_{mn} \end{bmatrix} \cdot \begin{bmatrix} E_1 \\ E_2 \\ \vdots \\ E_n \end{bmatrix} \tag{1}$$

Where, X represents the spectrum of X-ray, E denotes the electron spectrum and k_{ij} represents the relative contribution of the i-th electron interval to the production of X-ray in the j-th interval. The column j of the matrix K is the X-ray spectrum that is generated by the j-th electron interval.

2.2. Solution of the matrix equation

By having the X-ray spectrum and the coefficients matrix, equation (1) is solved and the electron spectrum is obtained. However, in solving this equation, due to the large condition number of the matrix K, the error in X is propagated by a very large factor in E, and the result will differ greatly from the true electron spectrum.

The condition number of a transformation matrix is a measure of output change for a small change in input. This parameter determines the error generated in E as the result of the existence of a certain value of error in X. Generally, if the condition number is k, the error may be propagated by k time; but this does not mean the exact amount of the error and only estimates the maximum error value. The important point here is that this error propagation is not related to the problem solving method, or the calculable number of decimal digits in the code, or the rounding error, and is merely the property of the matrix. A problem with a small condition number is a well-conditioned problem and the problem with a large condition number is called ill-conditioned.

Geometrically, a matrix is well-conditioned and has a condition number close to one, when its rows in the n-dimensional space form vectors approximately perpendicular to each other and in another case, a matrix is ill-conditioned and has a large condition number when its rows in n-dimensional space form approximate parallel vectors.

Physically, the ill-conditioning occurs when the X-ray spectrum obtained from two electron energy intervals are very close in form and intensity. In this case, given that there is an error in the measurements, it is difficult to determine which X-ray spectrum corresponds to which electron interval.

Different techniques may be proposed to reduce the condition number of coefficients matrix and increase the accuracy of the result. By decreasing the number of intervals of the electron spectrum, the condition numbers will also decrease. This is due to the fact that by reducing the number of electron intervals, the difference in the mean energy of the electron intervals also increases, and hence the difference of the X-ray spectrum of each interval will be larger. Of course, less details will be obtained from the spectrum by reducing the number of electron intervals. Another technique for reduction of the condition numbers is selection of an appropriate target material. By changing the target material, the characteristics of X-ray spectrum completely changes, and therefore the coefficients matrix K is also changed and the condition number will be different. We calculated the coefficients matrix for three target materials of aluminum, copper and tungsten, which have low, medium, and high atomic numbers respectively.

Some genetic algorithm-based methods and Monte Carlo methods were also proposed for reduction of condition number [17,18]. However in these methods the condition number of matrix K in $X = K \times E$ equation decreases, new X and E matrixes are generated with higher errors. Therefore, these methods do not help

to obtain the solution with lower error.

Generally, matrix solution did not indicate good performance in recovery of the electron spectrum. This is why alternative methods like neural network method can be considered here. It does not mean that the condition number of the coefficients matrix does not affects the accuracy of results in the neural network method, but under identical conditions, it produces more accurate results than matrix solution method.

2.3. Artificial neural network

Artificial Neural Networks (ANN) is a data processing system which processes data through many small processors that operate in a parallel network to solve the problem. In these networks, processor units are referred as neuron. After creating a network of these neurons, this network in trained by applying a training algorithm. Different types of artificial neural networks have been introduced, mainly used in applications such as classification, clustering, pattern recognition, modeling and approximation of functions, control, estimation and optimization. Finding the energy spectrum of electrons through an X-ray energy spectrum is in fact a sort of function approximation.

2.3.1. Multi-layer perceptron network

Multi-layer perceptron is a simple neural network which calculates only one output from real inputs by creating a linear combination based on weights of inputs and then applies a nonlinear transfer function on the output. Mathematical expression of this issue is shown in equation (2).

$$y = \phi\left(\sum_{i=1}^{n} w_i x_i + b\right) = \phi\left(w^T x + b\right) \tag{2}$$

Where w is the vector of weights, x is the input vector, b denotes the bias value and ϕ represents the transfer function. The transfer function is usually selected as a sigmoid or hyperbolic tangent. These functions are of concern due to their mathematical simplicity, and because their behavior is linear in the vicinity of the origin, and are saturated almost quickly when they are away from the origin. This selection makes the multi-layer perceptron capable of modeling both slight and severe non-linear fitting. A typical multi-layer perceptron consists of a set of input nodes that make up the input layer, one or more hidden layers (computing nodes), and output layer nodes. The input signal propagates layer-by-layer into the network. The number of hidden network layers can be selected. In Fig. 1, for example, the signal flow of such a network with one hidden layer is shown.

This neural network, which has one hidden layer, a nonlinear transfer function and a linear output layer, can be described as Equation (3).

$$x = f(s) = B\phi(As + a) + b \tag{3}$$

Where, s represents the vector of inputs, x denotes the vector of outputs, A is the matrix of the first-layer weights and a denotes bias vector of the first layer. B and b are weight matrix and the bias vector of the second layer, respectively. The function ϕ represents a nonlinear logical element. Performance of a multi-layer perceptron network with one hidden layer, as expressed in Equation (3), is surprisingly high. Multi-layer perceptron networks are commonly used for supervised learning problems. This means that there is a set of educational data in the form of input/output pairs and the network must learn the modeling of the relationship between them. Learning here means optimizing all weights and bias vectors (A, B, a, and b in Eq. (3)) for the sample pairs ($s(t)$, $x(t)$); so that the sum of the square of error $\left(\sum_t \left|\left|\boldsymbol{f}(s(t)) - x(t)\right|\right|^2\right)$ is minimized. This is performed by applying an optimization algorithm. In practical problems, it is necessary to select the properties of the network, such as the number of layers and the transfer function of each layer. It is even possible to create a separate network for each output.

2.3.2. Number of networks required

Given that the network output is the electron spectrum, the output has been consisted of a string of numbers, and so there are several outputs. In this case, we can create a specific network for each output, or for each output group. The criterion for choosing the number of networks is the connection between outputs. If the outputs are completely independent, creating several networks will provide a better result and if the outputs are dependent; a shared network will provide better solution. So, given that the outputs are dependent, we used only one network.

2.3.3. Number of hidden layers

It is optional to select one or more hidden layers for a multilayer perceptron network. In most cases, one hidden layer is usually sufficient, and in few cases, there is a need for two hidden layers. There is practically no need for three and more hidden layers. The electron spectrum and X-ray spectrum associated with it are linearly related; so, only one hidden layer is sufficient.

2.3.4. Number of neurons of layers

As shown in Fig. 1, the number of neurons in the output layer is equal to the number of network outputs. The number of neurons in the hidden layer (or layers) must be optimized. The low number of neurons causes the network's inability to approximate the function and the large number of neurons causes the lower accuracy of network's response. Although there is no general rule for determining the number of hidden layers, but approximate values for the upper and lower limits of the number of hidden layer can be estimated.

Each neuron aggregates all inputs with a specific weight and a bias value, and it applies a transfer function on it. These weights and the bias vectors are set in the training process, and are the unknowns of the hidden layer. If the number of neurons in the hidden layer is n_1 and the number of inputs is m, the number of unknowns of this layer is $(m + 1)n_1$. The output layer receives outputs of the hidden layer as inputs, and therefore its neuron number is equal to the number of network outputs. With the same argument, the number of unknowns of the output layer is $(n_1 + 1)n$.

If there are k samples for training, there are kn equations. To solve a problem, the number of equations must be greater than the number of unknowns. Therefore, we can conclude the following inequality:

$$(\mathrm{m}+1)n_1 + (n_1+1)n < kn \tag{4}$$

and rewrite Equation (4) as follows.

$$n_1 < \frac{(k-1)n}{(m+n+1)} \tag{5}$$

There is no rule in the case of lower limit of the number of neurons but experimentally, the number $2(m + n)$ of the neurons is proposed. Therefore, the limits of the number of neurons is as follows:

$$2(m+n) < n_1 < \frac{(k-1)n}{(m+n+1)} \tag{6}$$

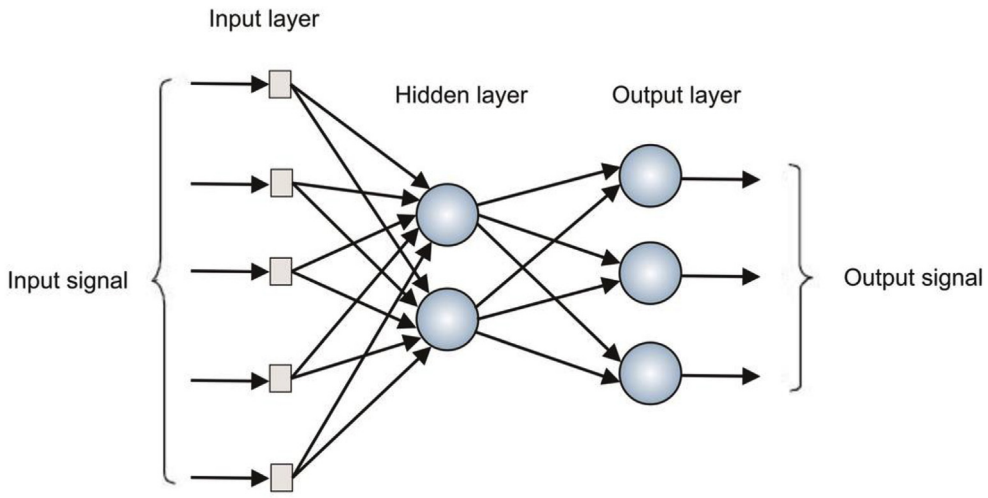

Fig. 1. Signal flow structure in multilayer perceptron network.

As it will be described in next sections, we used the MCNP code to produce training samples. There is no any limitation to produce the training samples (10^4 training samples were produced in this research) and therefore the upper limit of the inequality (6) is far from the usual number of neurons for such problems (~10). In the case of the lower limit; it is only a starting point to find the optimal number of neurons, and it is possible that the optimal number of neurons is also lower than the expressed value by inequality (6). In this research, after several trial solving of the problem we selected the number of 10 for the neurons in the hidden layer.

2.3.5. Transfer function

Each of the hidden layers and outputs have their specific transfer function. A list of transfer functions used in MATLAB software is presented in Table (1).

Since we use the network for the function approximation, the purelin function was selected as the output layer transfer function. Transfer functions of logsig, radbas, radbasn and tansig was selected for the hidden layer and responded well; but among these functions, the radbas function was selected.

2.4. Training artificial neural network

If we consider the electron spectrum as a point in the n-dimensional space as the input for network training, then this network must be trained in all regions of space using adequate number of training data. If the data does not include the entire space, in regions that the network is not trained, its response is probably false. If the number of data is low, the response will be less accurate. To satisfy this requirement we used a large number (~10^4) of low-energy, medium-energy, and high-energy electrons along with their own X-ray spectrum to train the network. In the training process, we assumed Gaussian single-peak electron spectrums (which is a common spectrum in most of pulsed electron generators) with different mean energies and different peak widths.

2.4.1. Calculation of the X-ray spectrum by the MCNP code

The X-ray spectrum resulting from the collision of any electron spectrum with the target at the desired geometry can be calculated using the MCNP code. MCNP is a Monte Carlo based code, which its calculation accuracy depends on the run time. Therefore, the uncertainty of the results can be reduced as low as required.

The geometry of X-ray generation by electron beam is simple. A source of mono-direction electrons perpendicularly hit a disk of copper. The copper is thick enough (2 cm) to stop the highest energy electrons. The X-ray detector is placed perpendicular to the direction of the electrons.

Table 1
List of widely used transfer functions available in MATLAB.

Explanation	Function
Log-sigmoid transfer function	logsig
Linear transfer function	purelin
Radial basis transfer function	radbas
Normalized radial basis transfer function	radbasn
Hyperbolic tangent sigmoid transfer function	tansig

A common problem with the use of neural networks is the lack of sufficient data to train the network. We used the superposition principle along with the MCNP code to produce training data. The transformation matrix was determined by calculating the X-ray spectrum resulting from each electron interval, separately, and using the fact that the *j-th* column of the transformation matrix is the X-ray spectrum that is generated by the *j*-th electron interval. Having the transformation matrix, by applying each assumed electron spectrum to equation (1), the corresponding X-ray spectrum is obtained.

The X-ray spectrums for network training are calculated by the MCNP code with uncertainty as low as we like. It means that if we apply an X-ray spectrum that is produced by MCNP to the network input, the network can recover the same electron spectrum which generated the X-ray. The lower the uncertainty in calculating of the X-ray spectrum, the more similar the recovered electron spectrum to the true spectrum. It should be noted that the X-ray spectra measured by experimental methods have relatively high measurement errors and this errors propagates in the electron spectrum recovered by the network. Therefore, in the network validating process, in order to provide similar conditions to real experiments, a random error was added to each energy interval in the X-ray spectra generated by the MCNP code to examine the performance of the neural network in real situations.

2.4.2. Network training process

Multi-layer perceptron is commonly used for supervised learning. This means that, as the learning algorithm is applied, the learning process is continuously monitored and supervised. Network training is in fact the optimization of weights and biases,

so that the closest response to the corresponding output is obtained. Thus, network training is a kind of optimization. The network monitoring criterion is the difference between the output of the network and the true output. The data provided to train the network is divided into three parts which are: training data, validation data, and testing data. All the three groups of data should be uniformly selected from entire areas of space. Otherwise, the accuracy of the network response will decrease. For this purpose, interleaved indices method were used.

Training data is known for the network and is used only for network training. Testing data are unknown for the network and is used at the end of the training process only for network testing. Validation data is also unknown for the network but with the difference that it's used in the training process and, its purpose is to monitor the learning process. In each step, an input/output pair of the training data is applied to train the network and weights are adjusted. Then the outputs obtained from the network are compared with the actual outputs. A validation data is used after a few training and, if an increase is observed in the network error in several consecutive validations, the learning process is stopped.

If we use enough data for training, and use the X-ray spectrums which are calculated with low uncertainty (which is possible by using MCNP code and running with large number of particles), the neural network must recover the true electron spectrum. If the network could perform that, the training process is verified.

2.4.3. Network training algorithm

There are several algorithms in MATLAB software for network training. Given that the application is *function approximation*, three algorithms are presented for network training, as shown in Table (2).

In the function approximation, for networks including several hundred weights and fewer, the *Levenberg-Marquardt* algorithm has the fastest convergence. In many cases, this algorithm is able to find the lowest least squared error in comparison with other algorithms. With the increase in the number of weights, the advantage of this algorithm decreases and it requires more memory. The *Bayesian regularization* algorithm requires a lot of time, but it has a good response to the low number of inaccurate data. Because there is no limitation in the number of data, there is no need to use the *Bayesian regularization* algorithm. The Scaled *Conjugate Gradient* algorithm requires less memory. Considering that the network training in our application does not require much memory, it is not necessary to use the *Scaled Conjugate Gradient* algorithm. Finally, given that in the double-layer network there is 10 neurons in each layer on average, and each neuron has ten weighting factors, there are about 200 wt in this network which should be optimized; so the *Levenberg-Marquardt* algorithm was selected for network training.

3. Results and discussions

3.1. Reducing the condition number by selecting the target material

Any change in the geometry and the experimental setup, such as the measurement angle and the target material will change the coefficients matrix. This change necessitates the re-production of inputs and retraining of the network for any geometry and layout. This means that the trained network for an experimental setup or a target material can only be used in the same setup or material.

Now, the question is that which material will result into the lowest condition number. Here the effect of three target materials of aluminum, copper and tungsten was studied. The condition numbers of the coefficients matrix for aluminum, copper and tungsten were calculated 3522, 1514, and 6345, respectively. In this research we selected copper as target material for estimation of electron spectrum, however it should be noted that sputtering of the copper surface by high current electron beam is much more serious than tungsten.

3.2. Results of the electron spectrum recovery

The X-ray spectrum resulted from collision of a pulsed electron beam to a target, can be measured by using a differential absorption spectrometry method with an error of less than 15% [19–21]. Therefore, in order to simulate the real conditions, a random error must be added to the X-ray spectra that are produced by MCNP. We evaluated the performance of the neural network for two different error values of maximum 3% and 10%. Main sources of error in X-ray spectra measurement are the statistical fluctuations of the number of particles as well as inaccuracy of the outputs of X-ray detector.

A number of electron spectra were selected and their corresponding X-ray spectra were calculated by MCNP code and the two error values were applied on the X-ray spectra. The electron spectrum was divided into ten intervals ranging 0–600 keV. Applying the 3% and 10% errors do not mean that all spectrum intervals have 3% or 10% of error. Rather, each interval randomly has an error in the range of 0–10% or 0–3%. After adding errors to the X-ray spectra, the electron spectra were recovered by the neural network and were compared with the true electron spectra. It took about one minute to recover each electron spectrum.

The comparison criterion for the recovered spectrum and the true spectrum is the standard difference that is calculated by equation (7).

$$S = \sqrt{\sum_{i=1}^{n} \left(C_i - C_i^{'}\right)^2} \tag{7}$$

Where, n is the number of electron energy intervals, C_i is the weight of i-th interval in the true spectrum, and C_i' is the weight of i-th interval in the recovered electron spectrum.

The results showed that the multi-layer perceptron network found the spectra with a good accuracy for both error values, and the recovered spectra have small difference with the true spectra. This difference is less than 10% of the values of the true spectrum for X-ray spectra whose components have the error value up to 3%. Fig. 2 shows three samples of the spectra recovered by the neural network with the true spectra. The standard difference between the two spectra in Fig. 2-a, 2-b and 2-c for the X-ray spectrum with a maximum error of 3% were 4.85%, 9.98% and 8.85% respectively and, for the X-ray spectrum with a maximum error of 10% were 13.07%, 12.72%, and 6.13%, respectively. As a result, if the general

Table 2
Three proposed algorithms for training of multi-layer perceptron network.

Characteristics	Full name of algorithm	Algorithm
Require more memory, Less time-consuming	Levenberg-Marquardt	trainlm
Time-consuming, but accurate response to the low number of data	Bayesian regularization	trainbr
Less memory is required	Scaled Conjugate Gradient	trainscg

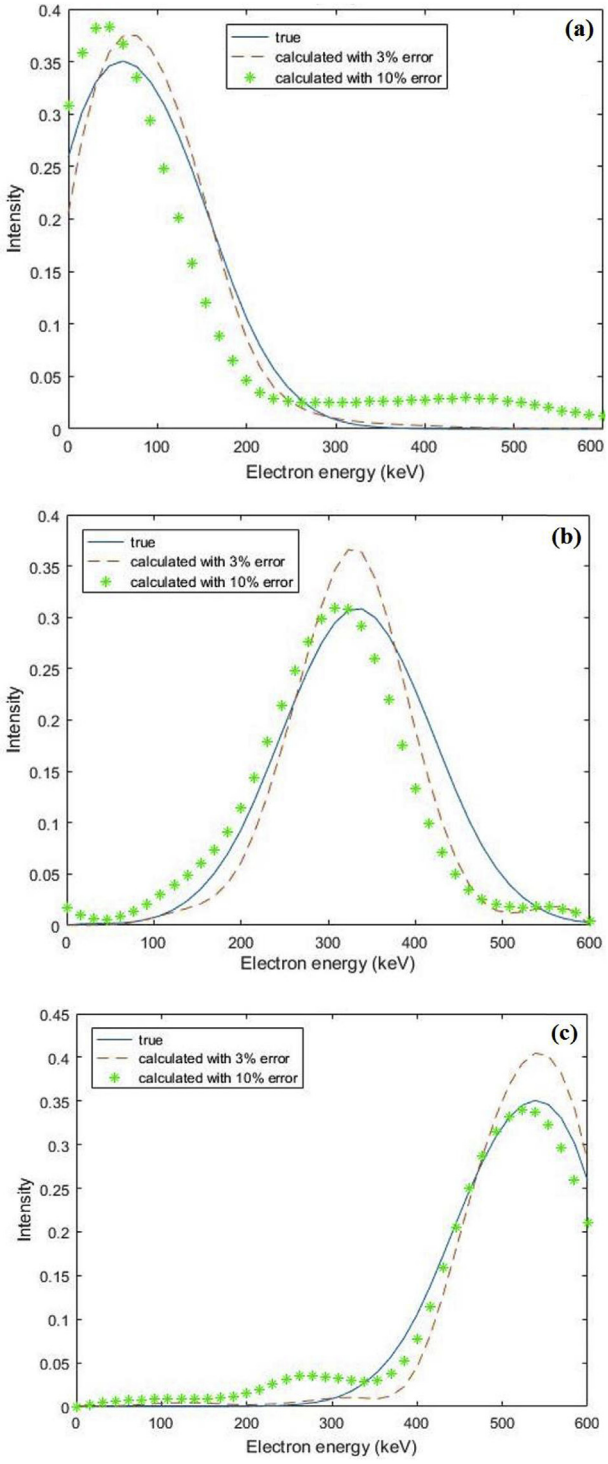

Fig. 2. The electron spectrum recovered by the neural network along with the true Gaussian spectrum (for the two maximum error values of 3% and 10% of the X-ray spectrum). (a) A low-energy peak; (b) A moderate-energy peak; and (c) A high-energy peak.

form of the electron spectrum is known (here, the Gaussian form), the multi-layer perceptron network, even with an error of nearly 10% of the X-ray spectrum, is able to recover the electron spectrum with acceptable accuracy.

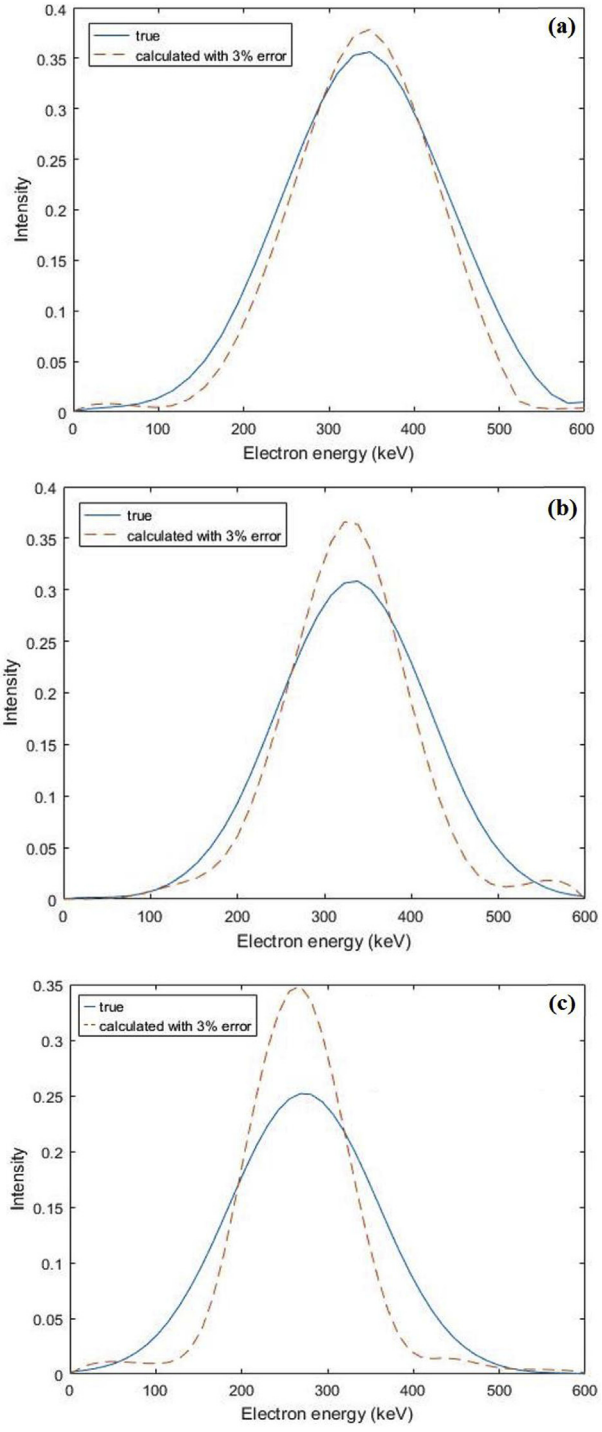

Fig. 3. The electron spectrum recovered by the neural network along with the true spectrum for different numbers of energy intervals (a) 8 intervals (b) 10 intervals and (c) 12 intervals.

3.3. Effect of the number of energy intervals on the accuracy of the spectrum recovery

By increasing the number of electron intervals, the X-ray spectra resulted from the individual electron intervals will have less difference and therefore the coefficients matrix will be more ill-conditioned. To investigate this, the recovery process was

performed for 8, 10 and 12 of electron intervals. As expected, network performance gets less accurate with increasing the number of electron intervals. Fig. 3 shows examples of recovered spectrum along with the true spectrum. The standard difference between the true and the recovered spectra in the examples shown in Fig. 3 for the 8, 10, and 12 intervals was calculated to be 6.49%, 9.98%, and 15.07%, respectively.

4. Conclusion

The proposed method is based on multilayer perceptron neural network for recovery of the electron spectrum from the X-ray spectrum resulting from collision of the electron beam with a target. The advantage of this method is that despite the adding 10% error to the X-ray spectrum, it recovered the true electron spectrum with about 11% relative error. For the X-ray spectrum with a maximum error of 3% and 10%, the multi-layer perceptron network estimated the electron spectrum in ten energy intervals with standard differences of 8% and 11%.

It is possible to obtain an electron spectrum in a more detailed way (that is, with higher numbers of intervals) but with lower accuracy. Finding the electron spectrum with higher accuracy is conditional on the measurement of the X-ray spectrum with less error.

This method can be used to recover the electron spectrum of pulsed electron beam generators such as plasma focus devices, induction linear accelerators as well as other devices in which there is not direct access to the electron beam and therefore direct electron spectroscopy is not possible, such as Tokamaks.

Declaration of competing interest

The authors declare that they have no known competing financial interests or personal relationships that could have appeared to influence the work reported in this paper.

References

[1] A.C. Patran, Electron and Medium Energy X-Ray Emission from a Dense Plasma Focus, National Institute of Education, Nanyang Technological University. PhD., 2002.
[2] M. Scholz, B. Bienkowska, V. Gribkov, R. Miklaszewski, Plasma focus as a source of intense radiation and plasma streams for technological applications, Acta Phys. Slovaca 54 (2004) 35–42.
[3] C. Moreno, M. Venere, R. Barbuzza, M. Del Fresno, R. Ramos, H. Bruzzone, F. Gonzalez, A. Clausse, Industrial applications of plasma focus radiation, Braz. J. Phys. 32 (1) (2002) 20–25.
[4] M. Sumini, L. Isolan, M. Cremonesi, C. Garibaldi, A Plasma Focus device as ultra-high dose rate pulsed radiation source. Part I: primary electron beam characterization, Radiat. Phys. Chem. 162 (2019) 1–11.
[5] E. Ceccolini, F. Rocchi, D. Mostacci, M. Sumini, A. Tartari, A range-based method to calibrate a magnetic spectrometer measuring the energy spectrum of the backward electron beam of a plasma focus, Rev. Sci. Instrum. 82 (2011), 085103.
[6] E. Ceccolini, Development and Performance Assessment of a Plasma Focus Electron Beam Generator for Intra-operative Radiation Therapy, Bologna University. PhD., 2012.
[7] R. Kwiatkowski, E. Skladnik-Sadowska, K. Malinowski, M.J. Sadowski, K. Czaus, J. Zebrowski, L. Karpinski, M. Paduch, M. Scholz, I.E. Garkusha, Measurements of electron and ion beams emitted from the PF-1000 device in the upstream and downstream direction, Nukleonika 56 (2011) 119–123.
[8] A. Patran, L. Tan, D. Stoenescu, M. Rafique, R. Rawat, S. Springham, T. Tan, P. Lee, M. Zakaullah, S. Lee, Spectral study of the electron beam emitted from a 3 kJ plasma focus, Plasma Sources Sci. Technol. 14 (2005) 549.
[9] A. Patran, D. Stoenescu, R. Rawat, S. Springham, T. Tan, L. Tan, M. Rafique, P. Lee, S. Lee, A magnetic electron analyzer for plasma focus electron energy distribution studies, J. Fusion Energy 25 (2006) 57–66.
[10] W. Stygar, G. Gerdin, F. Venneri, J. Mandrekas, Particle beams generated by a 6–12.5 kJ dense plasma focus, Nucl. Fusion 22 (1982) 1161.
[11] N. Neog, S. Mohanty, Study on electron beam emission from a low energy plasma focus device, Phys. Lett. 361 (2007) 377–381.
[12] W. Surała, M.J. Sadowski, R. Kwiatkowski, L. Jakubowski, J. Żebrowski, Measurements of fast electron beams and soft X-ray emission from plasma-focus experiments, Nukleonika 61 (2016) 161–167.
[13] H. Van Paassen, R. Vandre, R.S. White, X-ray spectra from dense plasma focus devices, Phys. Fluids 13 (1970) 2606–2612.
[14] C.M. Johns, R. Lin, The derivation of parent electron spectra from bremsstrahlung hard X-ray spectra, Sol. Phys. 137 (1992) 121–140.
[15] N. Shamsian, B. Shirani bidabadi, H. Pirjamadi, Development of a radiographic method for measuring the discrete spectrum of the electron beam from a plasma focus device, Plasma Sci. Technol. 19 (2017), 075101.
[16] A. Sharghi ido, M. Bonyadi, G. Etaati, M. Shahriari, Unfolding the neutron spectrum of a NE213 scintillator using artificial neural networks, Appl. Radiat. Isot. 67 (2009) 1912–1918.
[17] B. Fathi-Vajargah, M. Moradi, Diagonal scaling of ill-conditioned matrixes by genetic algorithm, J. Appl. Math. Stat. Inf. 8 (2012) 49–53.
[18] B. Fathi-Vajargah, M. Moradi, M. Kanafchian, Monte Carlo optimization for reducing the condition number of ill conditioned matrices, Adv. Comput. Math. Appl. (2012) 169–173.
[19] V. Raspa, C. Moreno, Radiographic method for measuring the continuum hard X-ray output spectrum of a Plasma Focus device, Phys. Lett. 373 (2009) 3659–3662.
[20] S.M. Miremad, B. Shirani, Measurement of the effective energy of pulsed X-rays emitted from a Mather-type plasma focus device, Appl. Radiat. Isot. 125 (2017) 169–175.
[21] S.M. Miremad, B. Shirani, Improvement of the radiographic method for measurement of effective energy of pulsed X-ray emission from a PF device for different anode's insert materials, Appl. Radiat. Isot. 136 (2018) 21–26.